IEEE Access
Multidisciplinary | Rapid Review | Open Access Journal

Received December 20, 2020, accepted December 30, 2020, date of publication January 8, 2021, date of current version January 20, 2021.

Digital Object Identifier 10.1109/ACCESS.2021.3050309

Wireless Sensor Network Localization Using AoA Measurements With Two-Step Error Variance-Weighted Least Squares

FUTA WATANABE, (Member, IEEE)
Information Technology R&D Center, Mitsubishi Electric Corporation, Kanagawa 247-8501, Japan
e-mail: watanabe.futa@ab.mitsubishielectric.co.jp

ABSTRACT We propose a novel localization method using angle-of-arrival (AoA) measurements with two-step error variance-weighted least squares (TELS). The first step is to estimate a terminal location provisionally using least squares. The second step is to estimate the terminal location using weighted least squares, with the weights for each anchor and each evaluation-function term, calculated from the error variance based on the first step. The proposed method does not require previous information on the environment while achieving high performance. The simulation results indicate that a root mean square error (RMSE) of the proposed method is superior to that of the existing hybrid received signal strength (RSS)/AoA localization methods. When 11 anchors are deployed inside a cube with edge length 15 m, and the standard deviations of measurements are small, the RMSE of the proposed method reaches about 0.34 m. It is nearly equal to that of Cramer-Rao lower bound (CRLB) on AoA.

INDEX TERMS Angle-of-arrival (AoA), received signal strength (RSS), localization, error variance, least squares (LS), wireless sensor networks (WSN).

I. INTRODUCTION

With the development of location-based services for smartphones and other devices in recent years, localization methods that use wireless sensor networks (WSNs) have been attracting considerable attention [1]–[6]. Among the range-based methods, received signal strength (RSS), time of flight (ToF), time of arrival (TOA), and time difference of arrival (TDoA) are the common measurements employed to estimate location [7]–[10]. Among the methods that do not require range information, proximity detection, fingerprint matching, and angle-of-arrival (AoA) measurements are common [11]–[16]. AoA-based localization methods are highly accurate, and various ways have been studied [14]–[16].

Hybrid localization methods that combine estimations from RSS and AoA measurements have been studied for high localization accuracy [1], [2], [17]–[20]. A localization problem is formulated as an optimization problem, and usually solved by least squares (LS). The weights based on the error covariance matrix [weighted linear least squares (WLLS)] were proposed to improve localization accuracy using the least squares [17]. Although this method achieves high localization accuracy, it is considered impractical as it requires that the standard deviations of RSS and AoA measurements, as well as the path-loss exponent, be known in advance. Moreover, the WLLS method decreases localization accuracy as RSS measurements greatly vary depending on individual differences in devices and environmental factors. Another technique introduced weights based on distance from a terminal [weighted least squares (WLS)] [18]. This relatively simple method is more accurate than other localization methods; however, it is also considered impractical due to the requirement that the RSS is measured in the environment in advance to calculate the path-loss exponent. Moreover, there is a possibility to improve localization accuracy because the weights are not optimized.

In this article, an accurate localization method that uses only AoA measurements and does not require previous information on the environment is proposed. To solve the optimization problem, we use a two-step error variance-weighted least squares (TELS) method. The first step is to estimate a terminal location provisionally using the least squares. Then, the second step is to estimate the terminal location using

The associate editor coordinating the review of this manuscript and approving it for publication was Wuliang Yin.

the weighted least squares, with the weights for each anchor and each evaluation-function term, calculated from the error variance based on the first step. This two-step process attenuates the effects of anchors and evaluation-function terms with large uncertainty to improve localization accuracy.

The main contributions of this article are as follows:

- A novel localization method using AoA measurements with the TELS is proposed. The proposed method does not require previous information on the environment.
- We present that the proposed method's computational complexity is equivalent to that of the existing hybrid RSS/AoA localization methods, solving the optimization problem in linear time.
- The simulation results indicate that the proposed method is superior to the existing hybrid RSS/AoA localization methods. Furthermore, in the case the standard deviations of measurements are small, the proposed method can achieve performance almost comparable to the Cramer-Rao lower bound (CRLB) on AoA.

The remainder of this article is organized as follows. Section II describes the problem formulation used in hybrid RSS/AoA localization methods to compare the proposed method with the existing ones. Section III describes the related works. Section IV presents the details of the proposed method. Section V describes the simulation results. Section VI discusses the proposed method, and finally, Section VII concludes this article.

In this article, italics denote scalars, lower-case boldface denotes vectors, $\mathbb{R}^N$ denotes vectors with N components, upper-case boldface denotes a matrix, $\mathbb{R}^{M\times N}$ denotes a M-by-N matrix, diag($\mathbf{a}$) denotes the diagonal matrix with $\mathbf{a}$ as the diagonal elements, $E(a)$ denotes the expected value of a, $V(a)$ denotes the variance of a and $\mathbf{I}_N$ denotes a N-by-N identity matrix.

II. PROBLEM FORMULATION

We assume a 3D space and an ideal line-of-sight (LOS) environment. In the 3D space, there exist N anchors and one terminal (Fig. 1). The anchor location is defined as $\mathbf{a}_i = [x_i, y_i, z_i]^T \in \mathbb{R}^3$ for $i = 1, \ldots, N$. The terminal location is defined as $\mathbf{x} = [x, y, z]^T \in \mathbb{R}^3$. The true values of AoA are given by (1), where ϕ_i^o is a true azimuth angle, ψ_i^o is a true elevation angle, and $d_i = \|\mathbf{x} - \mathbf{a}_i\|$.

$$\begin{aligned} \phi_i^o &= \arctan\left(\frac{y - y_i}{x - x_i}\right) \\ \psi_i^o &= \arccos\left(\frac{z - z_i}{d_i}\right) \end{aligned} \tag{1}$$

The measurements of RSS and AoA are given by (2), where ϕ_i are azimuth angle measurements, ψ_i are elevation angle measurements, and P_i are RSS measurements. P_0 is the RSS at a reference distance $d_0 (d_i \geq d_0)$, and γ_i is the path-loss exponent. n_{ϕ_i}, n_{ψ_i} and n_{P_i} are modeled as zero-mean Gaussian random variables with standard deviations, σ_{ϕ_i}, σ_{ψ_i} and σ_{P_i}, respectively: $n_{\phi_i} \sim N(0, \sigma_{\phi_i}^2)$, $n_{\psi_i} \sim N(0, \sigma_{\psi_i}^2)$ and $n_{P_i} \sim N(0, \sigma_{P_i}^2)$. Let $E(n_{\phi_i}) = E(n_{\psi_i}) = E(n_{P_i}) = 0$,

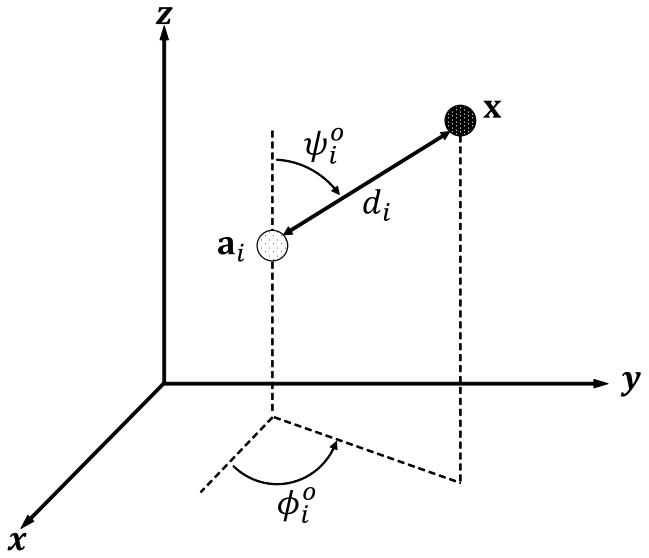

FIGURE 1. Illustration of anchor and terminal locations in the 3D space.

$E(n_{\phi_i}^2) = \sigma_{\phi_i}^2$, $E(n_{\psi_i}^2) = \sigma_{\psi_i}^2$, and $E(n_{P_i}^2) = \sigma_{P_i}^2$.

$$\begin{aligned} \phi_i &= \phi_i^o + n_{\phi_i} \\ \psi_i &= \psi_i^o + n_{\psi_i} \\ P_i &= P_0 - 10\gamma_i \log_{10}\frac{d_i}{d_0} + n_{P_i} \end{aligned} \tag{2}$$

III. RELATED WORKS

To achieve high localization accuracy, some researchers investigate hybrid localization methods using RSS and AoA measurements. A localization problem is formulated as an optimization problem and generally solved by the least squares. The WLLS [17] and the WLS [18] are known as the localization methods, achieving higher localization accuracy than the least squares. We describe the overview of these methods and the problem these methods have, as follows.

A. WEIGHTED LINEAR LEAST SQUARES (WLLS)

In [17], the authors applied weights to the linear least squares and considered the path loss exponent as an unknown variable. The RSS measurements were slightly different forms, as in (3).

$$P_i = P_0 - \gamma_i \nu \ln\frac{d_i}{d_0} + n_{P_i}, \tag{3}$$

where $\nu = \frac{10}{\ln 10}$. Then, the terminal location can be estimated by using the estimated distance $\hat{d}_i = d_0 \exp\left(\frac{P_0 - P_i}{\gamma \nu}\right)$, the azimuth angle measurements, ϕ_i, the elevation angle measurements, ψ_i, and unbiasing constants, δ_i and $\tilde{\delta}_i$, as in (4). Here, γ is the estimated pass-loss exponent.

$$\begin{aligned} \hat{x} &= x_i + \hat{d}_i \cos(\phi_i)\sin(\psi_i)\delta_i, \\ \hat{y} &= y_i + \hat{d}_i \sin(\phi_i)\sin(\psi_i)\delta_i, \\ \hat{z} &= z_i + \hat{d}_i \cos(\psi_i)\tilde{\delta}_i, \end{aligned} \tag{4}$$

where

$$\delta_i = \exp\left(\frac{\sigma_{\phi_i}^2 + \sigma_{\psi_i}^2}{2} - \frac{\sigma_{P_i}^2}{2(\gamma\nu)^2}\right),$$
$$\tilde{\delta}_i = \exp\left(\frac{\sigma_{\psi_i}^2}{2} - \frac{\sigma_{P_i}^2}{2(\gamma\nu)^2}\right).$$

By reformulating (4) into a vector form and applying the weighted linear least squares, the estimated location of the terminal, $\hat{\mathbf{x}}_{\mathrm{WLLS}}$, was given in (5).

$$\hat{\mathbf{x}}_{\mathrm{WLLS}} = \left(\mathbf{S}^T\mathbf{C}^{-1}\mathbf{S}\right)^{-1}\mathbf{S}^T\mathbf{C}^{-1}\bar{\mathbf{u}}, \tag{5}$$

where

$$\mathbf{S} = \begin{bmatrix} \mathbf{e}_N & \mathbf{0}_N & \mathbf{0}_N \\ \mathbf{0}_N & \mathbf{e}_N & \mathbf{0}_N \\ \mathbf{0}_N & \mathbf{0}_N & \mathbf{e}_N \end{bmatrix} \in \mathbb{R}^{3N\times 3},$$
$$\mathbf{C} = \begin{bmatrix} \mathbf{C}_{xx} & \mathbf{C}_{xy} & \mathbf{C}_{xz} \\ \mathbf{C}_{yx} & \mathbf{C}_{yy} & \mathbf{C}_{yz} \\ \mathbf{C}_{zx} & \mathbf{C}_{zy} & \mathbf{C}_{zz} \end{bmatrix} \in \mathbb{R}^{3N\times 3N},$$
$$\bar{\mathbf{u}} = \begin{bmatrix} x_1 + \hat{d}_1\cos(\phi_1)\sin(\psi_1)\delta_1 \\ \vdots \\ x_N + \hat{d}_N\cos(\phi_N)\sin(\psi_N)\delta_N \\ y_1 + \hat{d}_1\sin(\phi_1)\sin(\psi_1)\delta_1 \\ \vdots \\ y_N + \hat{d}_N\sin(\phi_N)\sin(\psi_N)\delta_N \\ z_1 + \hat{d}_1\cos(\psi_1)\tilde{\delta}_1 \\ \vdots \\ z_N + \hat{d}_N\cos(\psi_N)\tilde{\delta}_N \end{bmatrix} \in \mathbb{R}^{3N},$$

with $\mathbf{e}_N$ denotes column vectors of N ones and $\mathbf{0}_N$ denotes column vectors of N zeros, respectively. $\mathbf{C}$ denotes the covariance matrix. The elements of the covariance matrix are given in Appendix A. Although this method is accurate, it is considered impractical as it requires that the standard deviations of RSS and AoA measurements, and the path-loss exponent, be known in advance. The computational complexity is $\mathcal{O}(N)$ [18]. After this, we refer this method to as "WLLS" in the further text.

B. WEIGHTED LEAST SQUARES (WLS)

In [18], by resorting to spherical coordinates, vector $\mathbf{x} - \mathbf{a}_i$ was expressed as $\mathbf{x} - \mathbf{a}_i = d_i\mathbf{u}_i : d_i \geq 0, \|\mathbf{u}_i\| = 1$, for $i = 1, \ldots, N$. The unit vector, $\mathbf{u}_i$, was given by (6).

$$\mathbf{u}_i = [\cos(\phi_i)\sin(\psi_i), \cos(\phi_i)\sin(\psi_i), \cos(\psi_i)]^T \tag{6}$$

The authors presented the relations among the anchor location, the terminal location, the azimuth angle measurements, and the elevation angle measurements, as in (7), assuming that the standard deviations of measurements are sufficiently small.

$$\begin{aligned} \lambda_i\mathbf{u}_i^T(\mathbf{x} - \mathbf{a}_i) - \eta d_0 &\simeq 0, \\ \mathbf{c}_{1i}^T(\mathbf{x} - \mathbf{a}_i) &\simeq 0, \\ (\cos(\psi_i)\mathbf{u}_i - \mathbf{k})^T(\mathbf{x} - \mathbf{a}_i) &\simeq 0, \end{aligned} \tag{7}$$

where $\lambda_i = 10^{\frac{P_i}{10\gamma}}$, $\eta = 10^{\frac{P_0}{10\gamma}}$, $\mathbf{c}_{1i} = [-\sin(\phi_i), \cos(\phi_i), 0]^T$ and $\mathbf{k} = [0, 0, 1]^T$. The estimated location of the terminal, $\hat{\mathbf{x}}_{\mathrm{WLS}}$, is the solution to the minimum-value problem, as in (8).

$$\begin{aligned} \hat{\mathbf{x}}_{\mathrm{WLS}} = \arg\min_{\mathbf{x}} &\sum_{i=1}^{N}\left(\lambda_i\mathbf{u}_i^T(\mathbf{x} - \mathbf{a}_i) - \eta d_0\right)^2 \\ &+ \sum_{i=1}^{N}\left(\mathbf{c}_{1i}^T(\mathbf{x} - \mathbf{a}_i)\right)^2 \\ &+ \sum_{i=1}^{N}\left((\cos(\psi_i)\mathbf{u}_i - \mathbf{k})^T(\mathbf{x} - \mathbf{a}_i)\right)^2 \end{aligned} \tag{8}$$

By expressing (8) in matrix form, we obtain the closed-form solution, as in (9).

$$\hat{\mathbf{x}}_{\mathrm{WLS}} = \left(\tilde{\mathbf{A}}^T\tilde{\mathbf{W}}^{-1}\tilde{\mathbf{A}}\right)^{-1}\tilde{\mathbf{A}}^T\tilde{\mathbf{W}}^{-1}\tilde{\mathbf{b}}, \tag{9}$$

where

$$\tilde{\mathbf{A}} = \begin{bmatrix} \lambda_1\mathbf{u}_1^T \\ \vdots \\ \lambda_N\mathbf{u}_N^T \\ \mathbf{c}_{11}^T \\ \vdots \\ \mathbf{c}_{1N}^T \\ (\cos(\psi_1)\mathbf{u}_1 - \mathbf{k})^T \\ \vdots \\ (\cos(\psi_N)\mathbf{u}_N - \mathbf{k})^T \end{bmatrix} \in \mathbb{R}^{3N\times 3},$$
$$\tilde{\mathbf{W}} = \mathbf{I}_3 \otimes \mathrm{diag}(w_1, \ldots, w_N) \in \mathbb{R}^{3N\times 3N},$$
$$\tilde{\mathbf{b}} = \begin{bmatrix} \lambda_1\mathbf{u}_1^T\mathbf{a}_1 + \eta d_0 \\ \vdots \\ \lambda_N\mathbf{u}_N^T\mathbf{a}_N + \eta d_0 \\ \mathbf{c}_{11}^T\mathbf{a}_1 \\ \vdots \\ \mathbf{c}_{1N}^T\mathbf{a}_N \\ (\cos(\psi_1)\mathbf{u}_1 - \mathbf{k})^T\mathbf{a}_1 \\ \vdots \\ (\cos(\psi_N)\mathbf{u}_N - \mathbf{k})^T\mathbf{a}_N \end{bmatrix} \in \mathbb{R}^{3N}.$$

Here, the weights are inversely proportional to the distance from the terminal, w_i, as in (10).

$$w_i = 1 - \frac{\hat{d}_i}{\sum_{i=1}^{N}\hat{d}_i} \tag{10}$$

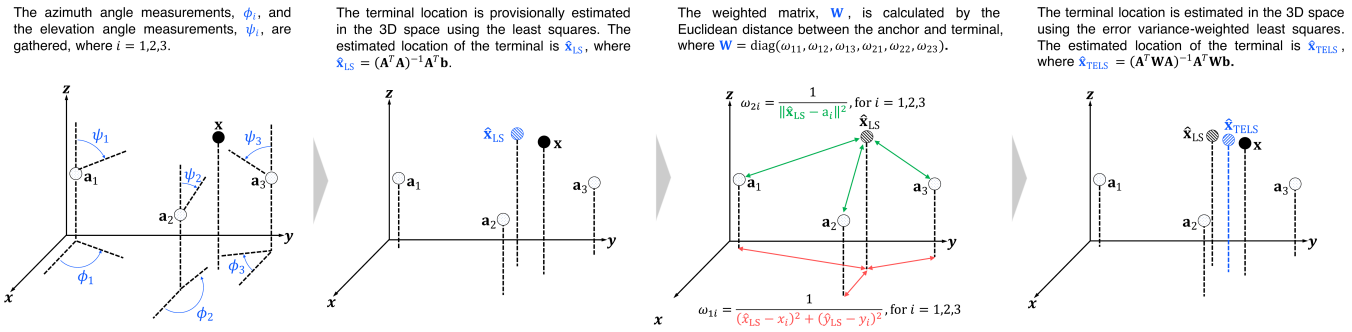

FIGURE 2. Flowchart of the two-step error variance-weighted least squares (TELS) method, when three anchors are deployed.

This method is accurate; however, it is also considered impractical due to the requirement that the RSS is measured in the environment in advance to calculate the path-loss exponent. Moreover, since the weights are not optimized, there is room for improvement. The computational complexity is $\mathcal{O}(N)$ [18]. After this, we refer this method to as "WLS" in the further text.

IV. PROPOTHED METHOD

This section describes the TELS method. Fig. 2 presents the flowchart of the proposed method. The proposed method uses only AoA measurements and does not require previous information on the environment, unlike the WLLS [17] and the WLS [18].

A. FIRST STEP: LEAST SQUARES LOCALIZATION

In the first step, the terminal location is provisionally localized in the 3D space using the least squares. Let the orthogonal vectors, $\mathbf{c}_{2i}$, for the relative position vector, $\mathbf{x} - \mathbf{a}_i$, be as in (11).

$$\mathbf{c}_{2i} = [\cos(\phi_i)\cos(\psi_i), \sin(\phi_i)\cos(\psi_i), -\sin(\psi_i)]^T \tag{11}$$

The product of $\mathbf{c}_{1i}$ and $\mathbf{x} - \mathbf{a}_i$, and the product of $\mathbf{c}_{2i}$ and $\mathbf{x} - \mathbf{a}_i$ are given by (12), which represent the relations among the anchor location, the terminal location, the azimuth angle measurements, and the elevation angle measurements. Here, ε_{1i} and ε_{2i} are errors which depend on the standard deviations of AoA measurements.

$$\begin{aligned} \mathbf{c}_{1i}^T(\mathbf{x} - \mathbf{a}_i) &= \varepsilon_{1i} \\ \mathbf{c}_{2i}^T(\mathbf{x} - \mathbf{a}_i) &= \varepsilon_{2i} \end{aligned} \tag{12}$$

The estimated location of the terminal, $\hat{\mathbf{x}}_{\mathrm{LS}}$, is the solution to the minimum-value problem, as in (13). Let $\hat{\mathbf{x}}_{\mathrm{LS}} = [\hat{x}_{\mathrm{LS}}, \hat{y}_{\mathrm{LS}}, \hat{z}_{\mathrm{LS}}]^T$.

$$\hat{\mathbf{x}}_{\mathrm{LS}} = \arg\min_{\mathbf{x}} \sum_{i=1}^{N} \left(\mathbf{c}_{1i}^T(\mathbf{x} - \mathbf{a}_i)\right)^2 + \sum_{i=1}^{N} \left(\mathbf{c}_{2i}^T(\mathbf{x} - \mathbf{a}_i)\right)^2 \tag{13}$$

By expressing (13) in matrix form, we obtain the closed-form solution, as in (14).

$$\hat{\mathbf{x}}_{\mathrm{LS}} = \left(\mathbf{A}^T\mathbf{A}\right)^{-1}\mathbf{A}^T\mathbf{b}, \tag{14}$$

where

$$\mathbf{A} = \begin{bmatrix} \mathbf{c}_{11}^T \\ \vdots \\ \mathbf{c}_{1N}^T \\ \mathbf{c}_{21}^T \\ \vdots \\ \mathbf{c}_{2N}^T \end{bmatrix} \in \mathbb{R}^{2N\times 3}, \quad \mathbf{b} = \begin{bmatrix} \mathbf{c}_{11}^T\mathbf{a}_1 \\ \vdots \\ \mathbf{c}_{1N}^T\mathbf{a}_N \\ \mathbf{c}_{21}^T\mathbf{a}_1 \\ \vdots \\ \mathbf{c}_{2N}^T\mathbf{a}_N \end{bmatrix} \in \mathbb{R}^{2N}.$$

After this, we refer this method to as "LS" in the further text.

B. SECOND STEP: ERROR VARIANCE-WEIGHTED LEAST SQUARES LOCALIZATION

In the second step, we add weights to the least squares, which are calculated from the error variance. Assuming that $|n_{\phi_i}|$ and $|n_{\psi_i}| \ll 1$, and employing geometric relations and additive theorems for trigonometric functions, (12) can be transformed into (15), where r_i denotes the Euclidean distance between the anchor and the terminal in the x and y planes, and d_i denotes the Euclidean distance between the anchor and the terminal in the 3D space. By giving the orthogonal vectors, $\mathbf{c}_{1i}$, as in (7), and $\mathbf{c}_{2i}$, as in (11), the errors can be expressed in terms of the Euclidean distance and the standard deviation alone.

$$\begin{aligned} \varepsilon_{1i} &= -(x - x_i)\sin(\phi_i) + (y - y_i)\cos(\phi_i) \\ &= -\sin(n_{\phi_i})((x - x_i)\cos(\phi_i^o) + (y - y_i)\sin(\phi_i^o)) \\ &\quad - \cos(n_{\phi_i})((x - x_i)\sin(\phi_i^o) - (y - y_i)\cos(\phi_i^o)) \\ &\cong -r_i n_{\phi_i}, \\ \varepsilon_{2i} &= (x - x_i)\cos(\phi_i)\cos(\psi_i) + (y - y_i)\sin(\phi_i)\cos(\psi_i) \\ &\quad - (z - z_i)\sin(\psi_i) \\ &\cong -\sin(n_{\psi_i})(r_i\sin(\psi_i^o) + (z - z_i)\cos(\psi_i^o)) \\ &\quad + \cos(n_{\psi_i})(r_i\cos(\psi_i^o) - (z - z_i)\sin(\psi_i^o)) \\ &\cong -d_i n_{\psi_i}, \end{aligned} \tag{15}$$

where $r_i = \sqrt{(x - x_i)^2 + (y - y_i)^2}$. The variances of ε_{1i} and ε_{2i} in (15) are calculated as in (16).

$$\begin{aligned} V(\varepsilon_{1i}) &= E((\varepsilon_{1i} - E(\varepsilon_{1i}))^2) = r_i^2 \sigma_{\phi_i}^2 \\ V(\varepsilon_{2i}) &= E((\varepsilon_{2i} - E(\varepsilon_{2i}))^2) = d_i^2 \sigma_{\psi_i}^2 \end{aligned} \tag{16}$$

Assuming that $\sigma_{\phi_i} \cong \sigma_{\psi_i}$, (16) can be expressed with a constant σ as in (17).

$$\begin{aligned} V(\varepsilon_{1i}) &\cong r_i^2 \sigma \\ V(\varepsilon_{2i}) &\cong d_i^2 \sigma \end{aligned} \tag{17}$$

To set the weights expressed in (18), we use the error variance, as in (17). The error variance is approximated using the anchor location, $\mathbf{a}_i$, and the estimated location of the terminal, $\hat{\mathbf{x}}_{\mathrm{LS}}$, obtained in the first step. By setting the weights as expressed in (18), the magnitudes of the error variance for each anchor and each evaluation-function term can be considered.

$$\begin{aligned} w_{1i} &= \frac{\sigma}{V(\varepsilon_{1i})} \cong \frac{1}{(\hat{x}_{\mathrm{LS}} - x_i)^2 + (\hat{y}_{\mathrm{LS}} - y_i)^2} \\ w_{2i} &= \frac{\sigma}{V(\varepsilon_{2i})} \cong \frac{1}{\|\hat{\mathbf{x}}_{\mathrm{LS}} - \mathbf{a}_i\|^2} \end{aligned} \tag{18}$$

The estimated location of the terminal, $\hat{\mathbf{x}}_{\mathrm{TELS}}$, is the solution to the minimum-value problem, as in (19). The weights attenuate the effects of anchors and evaluation-function terms with large uncertainty.

$$\begin{aligned} \hat{\mathbf{x}}_{\mathrm{TELS}} = \arg\min_{\mathbf{x}} & \sum_{i=1}^{N} w_{1i} \left(\mathbf{c}_{1i}^T (\mathbf{x} - \mathbf{a}_i) \right)^2 \\ & + \sum_{i=1}^{N} w_{2i} \left(\mathbf{c}_{2i}^T (\mathbf{x} - \mathbf{a}_i) \right)^2 \end{aligned} \tag{19}$$

By expressing (19) in matrix form, the closed-form solution is obtained as in (20).

$$\hat{\mathbf{x}}_{\mathrm{TELS}} = \left(\mathbf{A}^T \mathbf{W} \mathbf{A} \right)^{-1} \mathbf{A}^T \mathbf{W} \mathbf{b}, \tag{20}$$

where

$$\mathbf{W} = \mathrm{diag}(w_{11}, \ldots, w_{1N}, w_{21}, \ldots, w_{2N}) \in \mathbb{R}^{2N \times 2N}.$$

C. COMPLEXITY ANALYSIS

Table.1 presents the computational complexity of each method considered in this article. Table.2 presents the computational complexity of each operation used in the proposed method. Since the computation of the first step takes only $\mathcal{O}(N)$, and the computation of the second step also takes only $\mathcal{O}(N)$. Therefore, the proposed method's computational costs is $\mathcal{O}(N)$, as it does in existing methods. Since the computational complexity is linear time, the proposed method's computational complexity is sufficiently low for real-time applications.

TABLE 1. Computational Complexity of the Considered Method

Method	Description	Complexity
WLLS	WLLS in [17] based on RSS/AoA	$\mathcal{O}(N)$
WLS	WLS in [18] based on RSS/AoA	$\mathcal{O}(N)$
LS	Fisrs step of the proposed method based on AoA	$\mathcal{O}(N)$
TELS	Proposed method based on AoA	$\mathcal{O}(N)$

TABLE 2. Computational Complexity of Each Operation Used in the Proposed Method

Operation	Complexity
$\mathbf{A}$	$\mathcal{O}(N)$
$\mathbf{b}$	$\mathcal{O}(N)$
$\mathbf{A}^T\mathbf{A}$	$\mathcal{O}(N)$
$(\mathbf{A}^T\mathbf{A})^{-1}$	$\mathcal{O}(1)$
$(\mathbf{A}^T\mathbf{A})^{-1}\mathbf{A}^T$	$\mathcal{O}(N)$
$(\mathbf{A}^T\mathbf{A})^{-1}\mathbf{A}^T\mathbf{b}$	$\mathcal{O}(N)$
$\mathbf{W}$	$\mathcal{O}(N)$
$\mathbf{A}^T\mathbf{W}$	$\mathcal{O}(N)$
$\mathbf{A}^T\mathbf{W}\mathbf{A}$	$\mathcal{O}(N)$
$(\mathbf{A}^T\mathbf{W}\mathbf{A})^{-1}$	$\mathcal{O}(1)$
$(\mathbf{A}^T\mathbf{W}\mathbf{A})^{-1}\mathbf{A}^T$	$\mathcal{O}(N)$
$(\mathbf{A}^T\mathbf{W}\mathbf{A})^{-1}\mathbf{A}^T\mathbf{W}$	$\mathcal{O}(N)$
$(\mathbf{A}^T\mathbf{W}\mathbf{A})^{-1}\mathbf{A}^T\mathbf{W}\mathbf{b}$	$\mathcal{O}(N)$

TABLE 3. Simulation Conditions

Symbol	Description	Parameter
N	Number of anchors	$3, 4, 5, \ldots, 11$
$\mathbf{a}_i$	Anchor location	Randomly deployed inside a cube with edge length 15 m.
$\mathbf{x}$	Terminal location	Randomly deployed inside a cube with edge length 15 m.
σ_{ϕ_i}	Standard deviation of azimuth angle measurements	$2, 4, 6, 8, 10$ deg
σ_{ψ_i}	Standard deviation of elevation angle measurements	$2, 4, 6, 8, 10$ deg
σ_{P_i}	Standard deviation of RSS measurements	$2, 4, 6, 8, 10$ dBm
d_0	Reference distance	1 m
P_0	RSS at reference distance	$\mathcal{U}(-70, -40)$ dBm
γ_i	Path-loss exponent	$\mathcal{U}(1.57, 1.94)$
γ	Estimated path-loss exponent	1.7
M_c	Number of runs	50000

V. SIMULATION RESULTS

In this section, we present the results of numerical simulation to verify the proposed method's performance. Table.3 presents the simulation conditions with reference to [18], [21], [22]. All the measurements are generated by using (1) and (2). The terminal and anchors are randomly deployed inside a cube with edge length 15 m for each Monte Carlo run, with reference to [18]. The terminal is must be at least d_0 away from the anchors. The reference distance, d_0, is set to 1 m. We assume the LOS environment in the building and the 2.4 GHz band like Bluetooth Low Energy (BLE). The RSS at reference distance, P_0, is set to $\mathcal{U}(-70, -40)$ dBm, with reference to [21] because the RSS depends on the transmit power, the gain of transmit antenna, and the gain of receiver antenna. The path-loss exponent, γ_i, is set to $\mathcal{U}(1.57, 1.94)$, with reference to [22]. Since perfect knowledge of the path-loss exponent is practically impossible to obtain, the estimated path-loss exponent, γ, is set to 1.7. For our evaluation of

the simulation results, a root mean square error (RMSE) is calculated using (21), where $\hat{\mathbf{x}}(k)$ denotes the estimated location of the terminal for k-th Monte Carlo run, and M_c denotes the number of runs. The number of runs, M_c, is set to 50000. We compare the proposed method to the WLLS [17], the WLS [18], the LS and the CRLB on AoA (defined in Appendix B) [23], with the RMSE.

$$\text{RMSE} = \sqrt{\frac{1}{M_c}\sum_{k=1}^{M_c} \|\mathbf{x} - \hat{\mathbf{x}}(k)\|^2} \tag{21}$$

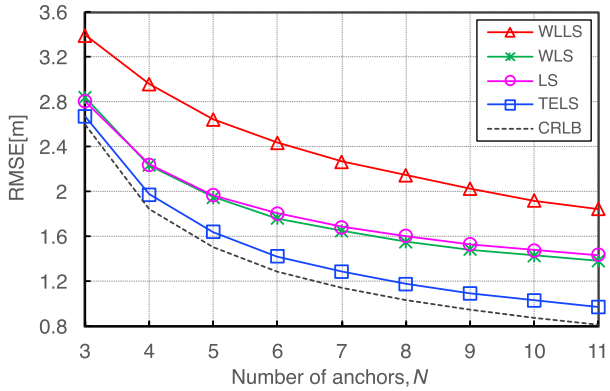

FIGURE 3. RMSE [m] of terminal localization versus the number of anchors, when $\sigma_{\phi_i} = 10$ deg, $\sigma_{\psi_i} = 10$ deg, and $\sigma_{P_i} = 6$ dBm.

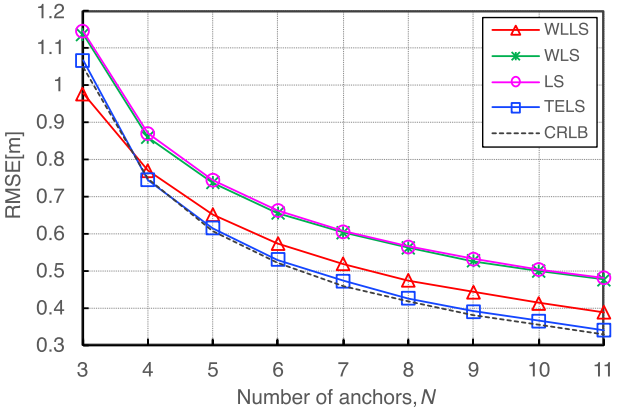

FIGURE 4. RMSE [m] of terminal localization versus the number of anchors, when $\sigma_{\phi_i} = 4$ deg, $\sigma_{\psi_i} = 4$ deg, and $\sigma_{P_i} = 2$ dBm.

A. DIFFERENT NUMBERS OF ANCHORS

Figure 3 illustrates the RMSE of the terminal localization versus the number of anchors when the standard deviations of measurements are large. In Fig. 3, the standard deviation of azimuth angle measurements, σ_{ϕ_i} is set to 10 deg, the standard deviation of elevation angle measurements, σ_{ψ_i} is set to 10 deg, and the standard deviation of RSS measurements, σ_{P_i} is set to 6 dBm. Figure 4 illustrates the RMSE of the terminal localization versus the number of anchors when the standard deviations of measurements are small. In Fig. 4, the standard deviation of azimuth angle measurements, σ_{ϕ_i} is set to 4 deg, the standard deviation of elevation measurements angle, σ_{ψ_i} is set to 4 deg, and the standard deviation of RSS measurements, σ_{P_i} is set to 2 dBm.

As presented in Fig. 3, when the standard deviations of measurements are large, the RMSE of the proposed method is the second smallest after the CRLB among all the methods, regardless of the number of anchors. As presented in Fig. 4, when the standard deviations of measurements are small, the RMSE of the proposed method is close to that of the CRLB. On the other hand, the RMSE of the proposed method is larger than that of the WLLS when only three anchors are deployed.

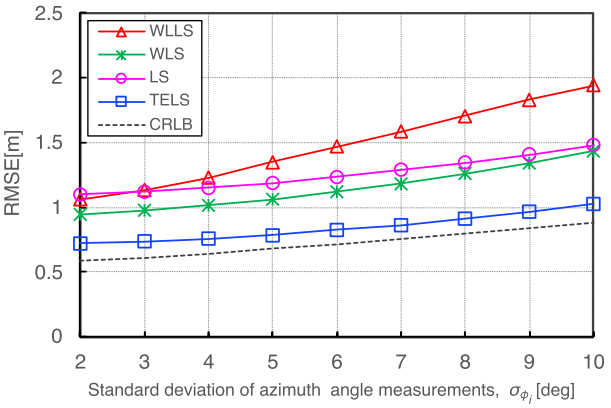

FIGURE 5. RMSE [m] of terminal localization versus the standard deviation of azimuth angle measurements [deg], when $N = 10$, $\sigma_{\psi_i} = 10$ deg, and $\sigma_{P_i} = 6$ dBm.

B. DIFFERENT STANDARD DEVIATIONS OF AZIMUTH ANGLE

Figure 5 illustrates the RMSE of the terminal localization versus the standard deviation of azimuth angle measurements. In Fig. 5, the number of anchors, N, is set to 10, the standard deviation of elevation angle measurements, σ_{ψ_i} is set to 10 deg, and the standard deviation of RSS measurements, σ_{P_i} is set to 6 dBm.

As presented in Fig. 5, the RMSE of the proposed method is the second smallest after the CRLB among all the methods, regardless of the standard deviation of azimuth angle measurements.

C. DIFFERENT STANDARD DEVIATIONS OF ELEVATION ANGLE

Figure 6 illustrates the RMSE of the terminal localization versus the standard deviation of elevation angle measurements. In Fig. 6, the number of anchors, N, is set to 10, the standard deviation of azimuth angle measurements, σ_{ϕ_i} is set to 10 deg, and the standard deviation of RSS measurements, σ_{P_i} is set to 6 dBm.

As presented in Fig. 6, the RMSE of the proposed method is the second smallest after the CRLB among all the

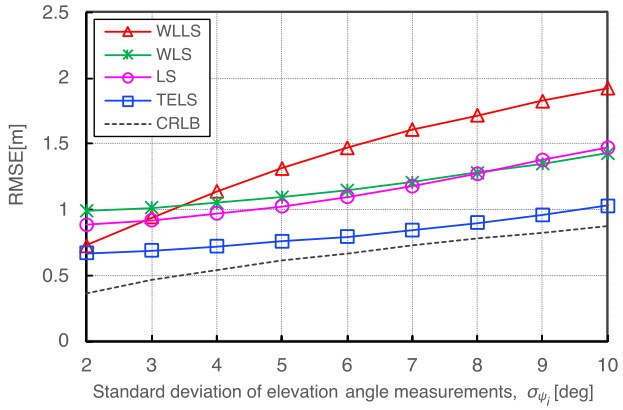

FIGURE 6. RMSE [m] of terminal localization versus the standard deviation of elevation angle measurements [deg], when $N = 10$, $\sigma_{\phi_i} = 10$ deg, and $\sigma_{P_i} = 6$ dBm.

methods, regardless of the standard deviation of elevation angle measurements.

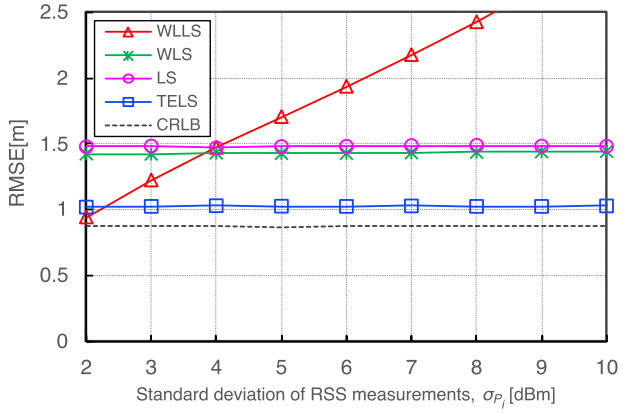

FIGURE 7. RMSE [m] of terminal localization versus the standard deviation of RSS measurements [dBm], when $N = 10$, $\sigma_{\phi_i} = 10$ deg, and $\sigma_{\psi_i} = 10$ deg.

D. DIFFERENT STANDARD DEVIATIONS OF RSS

Figure 7 illustrates the RMSE of the terminal localization versus the standard deviation of RSS measurements, σ_{P_i}. In Fig. 7, the number of anchors, N, is set to 10, the standard deviation of azimuth angle measurements, σ_{ϕ_i} is set to 10 deg, and the standard deviation of elevation angle measurements, σ_{ψ_i} is set to 10 deg.

As presented in Fig. 7, when the standard deviation of RSS measurements is greater than 2 dBm, the RMSE of the proposed method is the second smallest after the CRLB among all the methods. On the other hand, when the standard deviation of RSS measurements is 2 dBm, the RMSE of the proposed method is larger than that of the CRLB and WLLS. Since the TELS only uses the AoA measurements to estimate the terminal location, it is not affected by the standard deviation of RSS measurements. The RMSE is constant, regardless of the size of the standard deviation of RSS measurements.

VI. DISCUSSION

The simulation results indicate that the proposed method is more accurate than the existing hybrid RSS/AoA localization methods. Moreover, when the standard deviations of measurements are small, the RMSE of the proposed method is almost comparable to that of the CRLB. On the other hand, when the standard deviations of measurements are large, the RMSE of the proposed method is greater than that of the CRLB. This reason is considered that when the standard deviations of measurements are large, the difference between the approximated error variance of the proposed method and the actual error variance becomes large.

Since only AoA measurements are used, the method is not influenced by the environmental variances of RSS measurements. In the case of indoor localization in offices and shopping malls, since the anchors are likely to be placed in the LOS of the terminal, such as ceilings and walls, the proposed method can achieve high localization accuracy. Moreover, since the proposed method does not require previous information on the standard deviation of measurements and the path-loss exponent, it is practical to use if only the anchor location, the azimuth angle measurements, and the elevation angle measurements are available. Furthermore, the method's low computational cost makes it suitable for use in real-time, even on devices with relatively poor specifications.

The proposed method exhibits higher localization accuracy than the conventional WLS [18], as appropriate weights are set for each evaluation-function term that solves the problem on minimum-value. Since the WLS sets the same weights for each term, it does not account for the difference between the error variance of each term. For this reason, the localization accuracy deteriorates.

Since the proposed method assumes the same LOS environment as the existing methods, it will suffer reduced accuracy if the LOS is obstructed. In the proposed method, we assume that the standard deviation of azimuth angle measurements and that of elevation angle measurements are equal when the error variance is approximated. Therefore, when these standard deviations are different, localization accuracy will suffer. However, as presented in Figs. 5 and 6, when the standard deviations of azimuth and elevation angle measurements are between 0 deg and 10 deg, the localization accuracy is not significantly affected.

VII. CONCLUSION

With only AoA measurements, our TELS method achieves accurate 3D localization using the two-step optimization process. Its computational complexity is the same as that of the existing methods in linear time. The simulation results indicate that the proposed method can achieve higher localization accuracy than the existing hybrid RSS/AoA localization methods. Moreover, when the standard deviations of measurements are small, the proposed method can achieve performance nearly equivalent to the CRLB. The proposed method is simple, powerful, and computationally inexpensive, making it suitable for practical use in indoor environments.

The localization accuracy of the proposed method can be further improved. If the terminal is mobile, the method can be hybridized to the movement model of the terminal or the pedestrian dead reckoning (PDR). This extension of the method may also make it effective in non-line-of-site (NLOS) environments. Validation and improvement of the method to make it suitable for practical use will be the focus of future work. This step will require the evaluation using AoA-compliant radio modules in real environments.

APPENDIX A

The covariance matrix in the WLLS [17] is given by Equations (A1–A9).

$$\mathbf{C}_{xx} = \mathrm{diag}(\mathrm{C}_{xx_1}, \ldots, \mathrm{C}_{xx_N}) \in \mathbb{R}^{N\times N}, \tag{A1}$$

where

$$\begin{aligned}\mathrm{C}_{xx_i} &= \frac{\hat{d}_i^2}{4}\exp\left(\frac{\sigma_{P_i}^2}{(\gamma\nu)^2}+\sigma_{\phi_i}^2+\sigma_{\psi_i}^2\right)\\ &\quad-\frac{\hat{d}_i^2}{4}\cos(2\psi_i)\exp\left(\frac{\sigma_{P_i}^2}{(\gamma\nu)^2}+\sigma_{\phi_i}^2-\sigma_{\psi_i}^2\right)\\ &\quad+\frac{\hat{d}_i^2}{4}\cos(2\phi_i)\exp\left(\frac{\sigma_{P_i}^2}{(\gamma\nu)^2}-\sigma_{\phi_i}^2+\sigma_{\psi_i}^2\right)\\ &\quad-\frac{\hat{d}_i^2}{4}\cos(2\psi_i)\cos(2\psi_i)\exp\left(\frac{\sigma_{P_i}^2}{(\gamma\nu)^2}-\sigma_{\phi_i}^2-\sigma_{\psi_i}^2\right)\\ &\quad-\hat{d}_i^2\cos^2(\phi_i)\sin^2(\psi_i), \quad \text{for } i=1,\ldots,N.\end{aligned}$$

$$\mathbf{C}_{yy} = \mathrm{diag}(\mathrm{C}_{yy_1}, \ldots, \mathrm{C}_{yy_N}) \in \mathbb{R}^{N\times N}, \tag{A2}$$

where

$$\begin{aligned}\mathrm{C}_{yy_i} &= \frac{\hat{d}_i^2}{4}\exp\left(\frac{\sigma_{P_i}^2}{(\gamma\nu)^2}+\sigma_{\phi_i}^2+\sigma_{\psi_i}^2\right)\\ &\quad-\frac{\hat{d}_i^2}{4}\cos(2\psi_i)\exp\left(\frac{\sigma_{P_i}^2}{(\gamma\nu)^2}+\sigma_{\phi_i}^2-\sigma_{\psi_i}^2\right)\\ &\quad-\frac{\hat{d}_i^2}{4}\cos(2\phi_i)\exp\left(\frac{\sigma_{P_i}^2}{(\gamma\nu)^2}-\sigma_{\phi_i}^2+\sigma_{\psi_i}^2\right)\\ &\quad+\frac{\hat{d}_i^2}{4}\cos(2\psi_i)\cos(2\psi_i)\exp\left(\frac{\sigma_{P_i}^2}{(\gamma\nu)^2}-\sigma_{\phi_i}^2-\sigma_{\psi_i}^2\right)\\ &\quad-\hat{d}_i^2\sin^2(\phi_i)\sin^2(\psi_i), \quad \text{for } i=1,\ldots,N.\end{aligned}$$

$$\mathbf{C}_{zz} = \mathrm{diag}(\mathrm{C}_{zz_1}, \ldots, \mathrm{C}_{zz_N}) \in \mathbb{R}^{N\times N}, \tag{A3}$$

where

$$\begin{aligned}\mathrm{C}_{zz_i} &= \frac{\hat{d}_i^2}{2}\exp\left(\frac{\sigma_{P_i}^2}{(\gamma\nu)^2}+\sigma_{\psi_i}^2\right)\\ &\quad+\frac{\hat{d}_i^2}{2}\cos(2\psi_i)\exp\left(\frac{\sigma_{P_i}^2}{(\gamma\nu)^2}-\sigma_{\psi_i}^2\right)\\ &\quad-\hat{d}_i^2\cos^2(\psi_i), \quad \text{for } i=1,\ldots,N.\end{aligned}$$

$$\mathbf{C}_{xy} = \mathrm{diag}(\mathrm{C}_{xy_1}, \ldots, \mathrm{C}_{xy_N}) \in \mathbb{R}^{N\times N}, \tag{A4}$$

$$\mathbf{C}_{yz} = \mathrm{diag}(\mathrm{C}_{yz_1}, \ldots, \mathrm{C}_{yz_N}) \in \mathbb{R}^{N\times N}, \tag{A5}$$

where

$$\begin{aligned}\mathrm{C}_{xy_i} &= \mathrm{C}_{yx_i}\\ &= \frac{\hat{d}_i^2}{2}\sin(\phi_i)\cos(\psi_i)\\ &\quad\times\exp\left(\frac{\sigma_{P_i}^2}{(\gamma\nu)^2}-\sigma_{\phi_i}^2+\sigma_{\psi_i}^2\right)\\ &\quad-\frac{\hat{d}_i^2}{2}\sin(\phi_i)\cos(\psi_i)\cos(2\psi_i)\\ &\quad\times\exp\left(\frac{\sigma_{P_i}^2}{(\gamma\nu)^2}-\sigma_{\phi_i}^2+\sigma_{\psi_i}^2\right)\\ &\quad-\hat{d}_i^2\sin(\phi_i)\cos(\phi_i)\sin^2(\psi_i), \quad \text{for } i=1,\ldots,N.\end{aligned}$$

$$\mathbf{C}_{xz} = \mathrm{diag}(\mathrm{C}_{xz_1}, \ldots, \mathrm{C}_{xz_N}) \in \mathbb{R}^{N\times N}, \tag{A6}$$

$$\mathbf{C}_{zx} = \mathrm{diag}(\mathrm{C}_{zx_1}, \ldots, \mathrm{C}_{zx_N}) \in \mathbb{R}^{N\times N}, \tag{A7}$$

where

$$\begin{aligned}\mathrm{C}_{xz_i} &= \mathrm{C}_{zx_i}\\ &= \hat{d}_i^2\cos(\phi_i)\sin(\psi_i)\cos(\psi_i)\\ &\quad\times\exp\left(\frac{\sigma_{P_i}^2}{(\gamma\nu)^2}-\sigma_{\psi_i}^2\right)\\ &\quad-\hat{d}_i^2\cos(\phi_i)\sin(\psi_i)\cos(\psi_i), \quad \text{for } i=1,\ldots,N.\end{aligned}$$

$$\mathbf{C}_{yz} = \mathrm{diag}(\mathrm{C}_{yz_1}, \ldots, \mathrm{C}_{yz_N}) \in \mathbb{R}^{N\times N}, \tag{A8}$$

$$\mathbf{C}_{zy} = \mathrm{diag}(\mathrm{C}_{zy_1}, \ldots, \mathrm{C}_{zy_N}) \in \mathbb{R}^{N\times N}, \tag{A9}$$

where

$$\begin{aligned}\mathrm{C}_{yz_i} &= \mathrm{C}_{zy_i}\\ &= \hat{d}_i^2\sin(\phi_i)\sin(\psi_i)\cos(\psi_i)\\ &\quad\times\exp\left(\frac{\sigma_{P_i}^2}{(\gamma\nu)^2}-\sigma_{\psi_i}^2\right)\\ &\quad-\hat{d}_i^2\sin(\phi_i)\sin(\psi_i)\cos(\psi_i), \quad \text{for } i=1,\ldots,N.\end{aligned}$$

APPENDIX B

The Cramer-Rao lower bound (CRLB) [23] provides a theoretical lower bound on the variance of localization error, which is defined using the inverse of the Fisher information metric (FIM), $\mathbf{J}$. The relation between the FIM and the RMSE for the AoA-based localization is given by (B1).

$$\mathrm{RMSE} = \sqrt{\mathrm{trace}\left(\mathbf{J}^{-1}\right)}, \tag{B1}$$

where

$$\begin{aligned}\mathbf{J} &= \mathbf{H}\Sigma^{-1}\mathbf{H}^T \in \mathbb{R}^{3\times 3},\\ \mathbf{H} &= \begin{bmatrix}\mathbf{H}_\phi & \mathbf{H}_\psi\end{bmatrix} \in \mathbb{R}^{3\times 2N},\\ \Sigma &= \mathrm{diag}\left(\sigma_{\phi_i}^2\mathbf{I}_N, \sigma_{\psi_i}^2\mathbf{I}_N\right) \in \mathbb{R}^{2N\times 2N},\\ \mathbf{H}_\phi &= \frac{\partial\mathbf{h}_\phi^T}{\partial\mathbf{x}} \in \mathbb{R}^{3\times N},\\ \mathbf{H}_\psi &= \frac{\partial\mathbf{h}_\psi^T}{\partial\mathbf{x}} \in \mathbb{R}^{3\times N},\end{aligned}$$

$$\mathbf{h}_{\phi} = \begin{bmatrix} \arctan\left(\dfrac{y-y_1}{x-x_1}\right) \\ \vdots \\ \arctan\left(\dfrac{y-y_N}{x-x_N}\right) \end{bmatrix} \in \mathbb{R}^N,$$

$$\mathbf{h}_{\psi} = \begin{bmatrix} \arccos\left(\dfrac{z-z_1}{d_1}\right) \\ \vdots \\ \arccos\left(\dfrac{z-z_N}{d_N}\right) \end{bmatrix} \in \mathbb{R}^N.$$

REFERENCES

[1] S. Tomic, M. Beko, and R. Dinis, "Distributed RSS-AoA based localization with unknown transmit powers," *IEEE Wireless Commun. Lett.*, vol. 5, no. 4, pp. 392–395, Aug. 2016.
[2] S. Tomic, M. Beko, and R. Dinis, "3-D target localization in wireless sensor networks using RSS and AoA measurements," *IEEE Trans. Veh. Technol.*, vol. 66, no. 4, pp. 3197–3210, Apr. 2017, doi: 10.1109/TVT.2016.2589923.
[3] N. Salman, M. Ghogho, and A. H. Kemp, "Optimized low complexity sensor node positioning in wireless sensor networks," *IEEE Sensors J.*, vol. 14, no. 1, pp. 39–46, Jan. 2014, doi: 10.1109/JSEN.2013.2278864.
[4] Y. Zhao, Z. Li, B. Hao, and J. Shi, "Sensor selection for TDOA-based localization in wireless sensor networks with non-line-of-sight condition," *IEEE Trans. Veh. Technol.*, vol. 68, no. 10, pp. 9935–9950, Oct. 2019, doi: 10.1109/TVT.2019.2936110.
[5] D. Alshamaa, F. Mourad-Chehade, and P. Honeine, "Decentralized kernel-based localization in wireless sensor networks using belief functions," *IEEE Sensors J.*, vol. 19, no. 11, pp. 4149–4159, Jun. 2019, doi: 10.1109/JSEN.2019.2898106.
[6] F. Zafari, A. Gkelias, and K. K. Leung, "A survey of indoor localization systems and technologies," *IEEE Commun. Surveys Tuts.*, vol. 21, no. 3, pp. 2568–2599, 3rd Quart., 2019, doi: 10.1109/COMST.2019.2911558.
[7] M. Shalaby, M. Shokair, and N. W. Messiha, "RSS cooperative localization in WSNs operating in the millimeter bands," *Wireless Pers. Commun.*, vol. 115, no. 3, pp. 2327–2334, Dec. 2020, doi: 10.1007/s11277-020-07683-7.
[8] T. Wang, H. Ding, H. Xiong, and L. Zheng, "A compensated multi-anchors TOF-based localization algorithm for asynchronous wireless sensor networks," *IEEE Access*, vol. 7, pp. 64162–64176, 2019, doi: 10.1109/ACCESS.2019.2917505.
[9] Y. Gan, X. Cong, and Y. Sun, "Refinement of TOA localization with sensor position uncertainty in closed-form," *Sensors*, vol. 20, no. 2, p. 390, Jan. 2020, doi: 10.3390/s20020390.
[10] Y. Zou and H. Liu, "TDOA localization with unknown signal propagation speed and sensor position errors," *IEEE Commun. Lett.*, vol. 24, no. 5, pp. 1024–1027, May 2020, doi: 10.1109/LCOMM.2020.2968434.
[11] M. Kolakowski, "Improving accuracy and reliability of Bluetooth low-energy-based localization systems using proximity sensors," *Appl. Sci.*, vol. 9, no. 19, p. 4081, Sep. 2019, doi: 10.3390/app9194081.
[12] M. Li, L. Zhao, D. Tan, and X. Tong, "BLE fingerprint indoor localization algorithm based on eight-neighborhood template matching," *Sensors*, vol. 19, no. 22, p. 4859, Nov. 2019, doi: 10.3390/s19224859.
[13] L. Li, X. Guo, N. Ansari, and H. Li, "A hybrid fingerprint quality evaluation model for WiFi localization," *IEEE Internet Things J.*, vol. 6, no. 6, pp. 9829–9840, Dec. 2019, doi: 10.1109/JIOT.2019.2932464.
[14] R. Zhang, J. Liu, X. Du, B. Li, and M. Guizani, "AOA-based three-dimensional multi-target localization in industrial WSNs for LOS conditions," *Sensors*, vol. 18, no. 8, p. 2727, Aug. 2018, doi: 10.3390/s18082727.
[15] B. Yimwadsana, V. Serey, and S. Sanghlao, "Performance analysis of an AoA-based Wi-Fi indoor positioning system," in *Proc. 19th Int. Symp. Commun. Inf. Technol. (ISCIT)*, Ho Chi Minh City, Vietnam, Sep. 2019, pp. 36–41, doi: 10.1109/ISCIT.2019.8905238.
[16] Y. Sun, K. C. Ho, and Q. Wan, "Eigenspace solution for AOA localization in modified polar representation," *IEEE Trans. Signal Process.*, vol. 68, pp. 2256–2271, Mar. 2020, doi: 10.1109/TSP.2020.2981773.
[17] M. W. Khan, N. Salman, A. H. Kemp, and L. Mihaylova, "Localisation of sensor nodes with hybrid measurements in wireless sensor networks," *Sensors*, vol. 16, no. 7, pp. 1–16, Jul. 2016, doi: 10.3390/s16071143.
[18] S. Tomic, M. Beko, R. Dinis, and L. Bernardo, "On target localization using combined RSS and AoA measurements," *Sensors*, vol. 18, no. 4, pp. 1–25, 2018, doi: 10.3390/s18041266.
[19] S. Tomic, M. Marikj, M. Beko, R. Dinis, and N. Orfao, "Hybrid RSS-AoA technique for 3-D node localization in wireless sensor networks," in *Proc. Int. Wireless Commun. Mobile Comput. Conf. (IWCMC)*, Dubrovnik, Croatia, Aug. 2015, pp. 1277–1282, doi: 10.1109/IWCMC.2015.7289266.
[20] T. L. N. Nguyen, T. D. Vy, and Y. Shin, "An efficient hybrid RSS-AoA localization for 3D wireless sensor networks," *Sensors*, vol. 19, no. 9, p. 2121, May 2019, doi: 10.3390/s19092121.
[21] U. M. Qureshi, Z. Umair, and G. P. Hancke, "Evaluating the implications of varying Bluetooth low energy (BLE) transmission power levels on wireless indoor localization accuracy and precision," *Sensors*, vol. 19, no. 15, p. 3282, Jul. 2019, doi: 10.3390/s19153282.
[22] J. Miranda, R. Abrishambaf, T. Gomes, P. Goncalves, J. Cabral, A. Tavares, and J. Monteiro, "Path loss exponent analysis in wireless sensor networks: Experimental evaluation," in *Proc. 11th IEEE Int. Conf. Ind. Informat. (INDIN)*, Bochum, Germany, Jul. 2013, pp. 54–58, doi: 10.1109/INDIN.2013.6622857.
[23] S. K. Jayaweera, "Introduction to estimation theory," in *Signal Processing for Cognitive Radios*. Hoboken, NJ, USA: Wiley, 2015, pp. 132–163, doi: 10.1002/9781118824818.ch5.

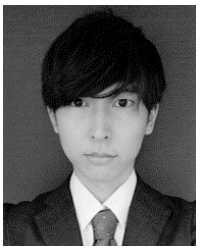

FUTA WATANABE (Member, IEEE) received the M.E. degree in space engineering from the Tokyo Institute of Technology, Tokyo, Japan, in 2017. In 2017, he joined Mitsubishi Electric Corporation, Tokyo, Japan, where he has been engaged in the research and development of wireless sensor networks, sensor localization, environment control, environment visualization, and autonomous service robot.